J|A|C|S
ARTICLES
Published on Web 10/11/2002

Electrochemical Sensing in Microfluidic Systems Using Electrogenerated Chemiluminescence as a Photonic Reporter of Redox Reactions

Wei Zhan, Julio Alvarez, and Richard M. Crooks*

Contribution from the Department of Chemistry, Texas A&M University, P.O. Box 30012, College Station, Texas 77842-3012

Received July 1, 2002

Abstract: This paper describes a microfluidics-based sensing system that relies on electrochemical detection and electrogenerated chemiluminescent (ECL) reporting. The important result is that the ECL reporting reaction is chemically decoupled from the electrochemical sensing reaction. That is, the electrochemical sensing reaction does not participate directly in the ECL process, but because electrochemical cells require charge balance, the sensing and ECL reactions are electrically coupled. This provides a convenient and sensitive means for direct photonic readout of electrochemical reactions that do not directly participate in an ECL reaction and thus broadens the spectrum of redox compounds that can be detected by ECL. The approach can be implemented in either a two-electrode or bipolar (single-electrode) configuration. By manipulating the placement and dimensions of the conductors, the photonic response can be enhanced. The system is used to electrochemically detect benzyl viologen present in solution and report its presence via $Ru(bpy)_3^{2+}$ (bpy = 2,2′-bipyridine) luminescence.

Introduction

Here, we report a microfluidics-based sensing system that relies on electrochemical detection and electrogenerated chemiluminescent (ECL)[1] reporting. The important new result is that the ECL reporting reaction is decoupled from the electrochemical sensing reaction. That is, the electrochemical sensing reaction does not participate directly in the ECL process, but because electrochemical cells require charge balance, the sensing and ECL reactions are electrically coupled. This provides a convenient and sensitive means for direct photonic readout of electrochemical reactions that do not directly participate in an ECL reaction and thus broadens the spectrum of redox compounds that can be detected by ECL. For convenience, we demonstrate this result using a microfluidic system configured with either a single bipolar electrode or with two electrodes connected to a power supply, but the approach is general and easily adaptable to any one- or two-compartment cell[2] containing one, two, or three electrodes.

In a conventional electrochemical experiment of the type sometimes used in chromatographic detectors, the potential of a working electrode is controlled with respect to that of a reference electrode, and the faradaic current flowing between the working electrode and an inert counter electrode is measured.[3] In this conventional approach, the entire information content of the system is provided by measuring current at the working electrode, and processes occurring at the counter electrode are nearly always ignored. One interesting aspect of the work described here is that the counter electrode plays a key role: it reports on processes occurring at the working electrode via ECL, which eliminates the need for a direct electrical measurement of the current. ECL was chosen as the reporter because of its analytical significance (high sensitivity, low cost, and low power consumption), but the approach would work equally well if the counter electrode activated any other photonic, magnetic, or chemical change that could be detected.

Particularly relevant to our work are findings recently reported by Manz and co-workers.[4] They described a microfluidic system configured to detect the presence of $Ru(bpy_3)^{2+}$ (bpy = 2,2′-bipyridine) and related light-emitting compounds, at a bipolar electrode via ECL. Although the arrangement of the experimental apparatus used in their work is similar to one of the electrochemical cells described here, the detection principle is different. Specifically, in the Manz approach, only analytes participating in the ECL reaction cascade at the anode were measured. They pointed out, however, that the current is expected to be limited by the limited availability of reducible substances.[4,5] In contrast, we use the anode reaction solely as an ECL reporter of events occurring at the cathode, where the analyte of interest is reduced.

As mentioned earlier, previous ECL studies have relied on the light-emitting species (the reporter) participating directly

* To whom correspondence should be addressed. E-mail: crooks@tamu.edu. Voice: 979-845-5629. Fax: 979-845-1399.

(1) Bard, A. J.; Faulkner, L. R. *Electrochemical Methods Fundamentals and Applications*, 2nd ed.; John Wiley & Sons: New York, 2000; Chapter 18 and references therein.
(2) Zhan, W.; Alvarez, J.; Crooks, R. M. *Anal. Chem.* **2002**, *74*, submitted.
(3) Bard, A. J.; Faulkner, L. R. *Electrochemical Methods Fundamentals and Applications*, 2nd ed.; John Wiley & Sons: New York, 2000; p 26.
(4) Arora, A.; Eijkel, J. C. T.; Morf, M. E.; Manz, A. A. *Anal. Chem.* **2001**, *73*, 3282−3288.
(5) Bard, A. J.; Faulkner, L. R. *Electrochemical Methods Fundamentals and Applications*, 2nd ed.; John Wiley & Sons: New York, 2000; p 439.

10.1021/ja020907s CCC: $22.00

in the chemistry of the detection process.[4,6−10] We demonstrate the principle of sensing an analyte that does not participate in the ECL reactions by detecting benzyl viologen (BV^{2+}) at the cathode and reporting its presence via luminescence arising from a previously reported complex reaction cascade that relies on electrooxidation of $Ru(bpy)_3^{2+}$ and a highly reducing coreactant generated in situ.[11] The coreactant used in this study is derived from oxidation of tripropylamine (TPA).[11,12]

Experimental Section

Chemicals. $Ru(bpy)_3Cl_2 \cdot 6H_2O$ (bpy = 2,2′-bipyridine) (minimum 98%) was purchased from Strem Chemicals (Newburyport, MA). Tripropylamine (TPA) (99+%) and benzyl viologen dichloride (BV^{2+}, 97%) were obtained from the Aldrich Chemical Co. (Milwaukee, WI). Deionized 18 MΩ·cm water (Milli-Q reagent water system, Millipore, Bedford, MA) was used to prepare all aqueous solutions. Unless otherwise noted, 0.1 M phosphate buffer (pH 6.9) was used as the supporting electrolyte solution for electrochemical measurements. All chemicals were used without further purification.

Device Fabrication. Standard lithographic and soft-lithographic methods[13] were used to prepare the indium tin oxide (ITO) microelectrodes and fabricate the microfluidic devices. Briefly, ITO-coated (thickness: ~200 nm, resistance: ~10 Ω/square) aluminosilicate glass slides (Delta Technologies, Ltd., Stillwater, MN) were first sonicated in a 1% detergent (Micro-90, International Products Co., Burlington, NJ) solution (1:4 (v/v) ethanolamine/water mixture) for 30 min and then dried. A positive photoresist layer (~15 μm thick, AZ P4620, Clariant Co., Somerville, NJ) was then spin coated onto this clean glass slide. Next, the photoresist layer was patterned by illuminating the resist with 365 nm light (EFOS Lite, UV spot lamp, Mississauga, Ontario) through a mask (photographic film) designed using a computer graphics program. These patterns were then transferred to the ITO layer by developing the photoresist and etching the ITO surface with an aqueous acid solution (5% HNO_3 and 20% HCl). The remaining photoresist was removed with acetone, and the patterned ITO electrodes on glass were then rinsed thoroughly with water and finally dried at 60 °C.

Microfluidic devices were prepared by a published method using poly(dimethylsiloxane) (PDMS, Dow Corning Sylgard Silicone Elastomer-184, Krayden, Inc.) molds.[13] The main channel of the device was 1.2 cm long, 750 μm wide, and 30 μm high. The PDMS devices were aligned over the patterned ITO-coated glass slides with the aid of an *x*,*y*,*z*-micropositioner (462 series, Newport Co., Irvine, CA) and a motion controller (model 861, Newport Co., Irvine, CA) under a microscope with a 10× lens (Optiphot, Nikon). The power supply used to carry out the experiments depended on the required voltage: (range 0−120 V, model LLS9120, Lambda; range 0−25 V, model E3620A, Hewlett-Packard). Electrical contacts were made to ITO using Ag paste (Epo-tek, Epoxy Technology, Billerica, MA). In the bipolar-electrode experiments, the electric field was generated by applying a current between two Ni wires (250 μm diameter) that were inserted into reservoirs present in PDMS molds. The one- and two-electrode configurations are compared in Scheme 1.

Electrochemical Measurements. Conventional three-electrode experiments were carried out using a Pine AFRDE4 bipotentiostat (Grove City, PA) and a Kipp and Zonen XYY′ chart recorder (Bohemia, NY). Clean ITO slides (Delta Technologies, Ltd., Stillwater, MN) were used as working electrodes with an approximate exposed area of 0.26 cm^2. In all cases, the counter electrode was a Pt wire, and the reference was Ag/AgCl (3 M NaCl) (Bioanalytical Systems, West Lafayette, IN). Solutions were not deaerated.

Scheme 1

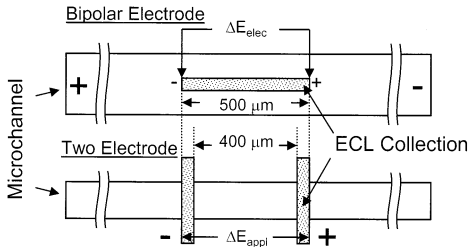

Scheme 2

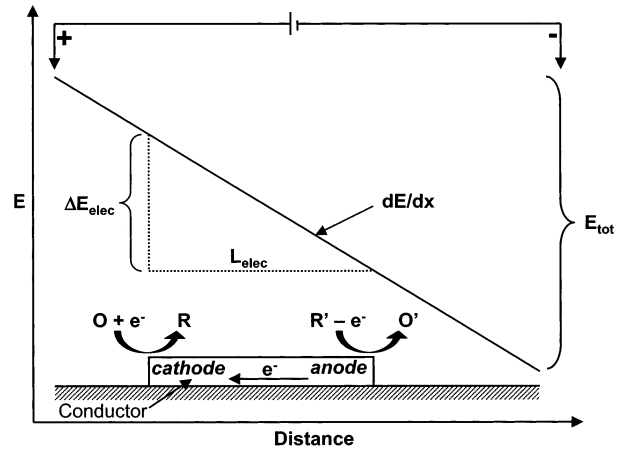

ECL Measurements. ECL spectra were acquired using a liquid nitrogen cooled, CCD-based (LN/CCD, Roper Scientific, Tucson, AZ) spectrometer (SpectraPro-300i, Acton Research Co., Acton, MA) under dark-room conditions. This spectrometer was connected to the side port of an optical/fluorescence-inverted microscope (ECLIPSE TE300, Nikon). The ECL acquisition time was typically 5 s with a slit width of 2 mm. To optimize the reproducibility of the ECL signal, the devices were refilled with fresh solution after each measurement. The run-to-run ECL variation was in the range of 5−10%. Solutions used to obtain ECL measurements were not deaerated.

Results and Discussion

Principle of Operation. Two different electrode configurations were used in this study (Scheme 1). The operation of the two-electrode system is straightforward. Electrical connections are made to the two electrodes, and a potential (ΔE_{appl}) is applied between them. If ΔE_{appl} reaches a critical value (E_{crit}), faradaic electrochemical processes will occur at both electrodes. In many cases, E_{crit} is roughly equal to the difference in the formal potentials of the redox processes occurring at the cathode ($E_c^{\circ\prime}$) and anode ($E_a^{\circ\prime}$). As in any electrochemical experiment, charge balance at the two electrodes is required, and thus an electrochemical process occurring at the cathode results in a process having an identical velocity at the anode. Our experiments are designed such that an ECL reaction occurs at the anode, and the photon flux is therefore related to the velocity of the cathode reaction.

The operation of a bipolar electrode is somewhat more complex, but it has been described extensively in the literature and therefore is only briefly summarized here.[4,14,15] The physical layout and energetics of the bipolar configuration used in our

(6) Arora, A.; de Mello, A. J.; Manz, A. *Anal. Commun.* **1997**, *34*, 393−395.
(7) Rubinstein, I.; Martin, C. R.; Bard, A. J. *Anal. Chem.* **1983**, *55*, 1580−1582.
(8) Blackburn, G. F.; Shah, H. P.; Kenten, J. H.; Leland, J.; Kamin, R. A.; Link, J.; Peterman, J.; Powell, M. J.; Shah, A.; Talley, D. B.; Tyagi, S. K.; Wilkins, E.; Wu, T.-G.; Massey, R. J. *Clin. Chem.* **1991**, *37*, 1534.
(9) Fahnrich, K. A.; Pravda, M.; Guilbault, G. G. *Talanta* **2001**, *54*, 531−559.
(10) Knight, A. W.; Greenway, G. M. *Analyst* **1994**, *119*, 879−890.
(11) Zu, Y.; Bard, A. J. *Anal. Chem.* **2000**, *72*, 3223−3232.
(12) Noffsinger, J. B.; Danielson, N. D. *Anal. Chem.* **1987**, *59*, 865−868.
(13) Xia, Y. N.; Whitesides, G. M. *Angew. Chem., Int. Ed.* **1998**, *37*, 550−575.

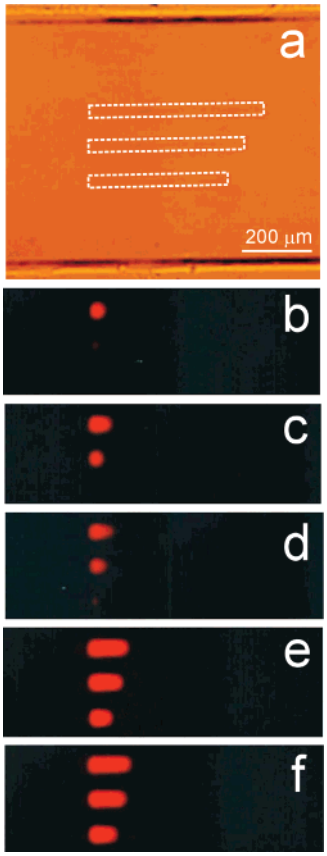

Figure 1. (a) Optical micrograph of the bipolar electrode configuration used to obtain the data in the other panels of this figure. Because the optical contrast between the ITO electrodes and the underlying glass substrates is low, the electrodes are outlined by dashed white lines. From top to bottom, the lengths of the electrodes are 500, 450, and 400 μm. (b−f) Luminescence micrographs showing the magnitude of ECL as a function of the voltage drop across the three electrodes. The calculated values of ΔE_{elec} and the value of E_{tot} for each electrode in each panel are provided in Table 1. The 0.1 M phosphate buffer electrolyte solution (pH 6.9) contained 5 mM $Ru(bpy)_3^{2+}$ and 25 mM TPA. The negative electrode used to apply E_{tot} was on the left.

experiments are summarized in Scheme 2. Here, L_{elec} is the length of the bipolar electrode, E_{tot} is the voltage across the solution in the microfluidic channel, and ΔE_{elec} is the fraction of E_{tot} dropped across the distance L_{elec}. If ΔE_{elec} exceeds E_{crit}, then faradaic processes will occur at both ends of the conductor. As for the two-electrode cell, the bipolar system is configured so that an ECL reaction cascade is the most energetically favorable process at the anode in the experiments reported below.

Effect of the Electrode Length on Wireless Electrochemical Reactions. Scheme 2 predicts that ΔE_{elec} depends on the electrode length and the potential gradient, dE/dx, along the fluidic channel. To confirm these expectations, we prepared three parallel ITO microelectrodes having lengths (L_{elec}, Scheme 2) of 400, 450, and 500 μm and configured as shown in Figure 1a. The electrodes were not connected to a potentiostat, and thus their potential was free to float. The main channel of the microfluidic device housing these three electrodes was filled with a solution containing 5 mM $Ru(bpy)_3^{2+}$ and 25 mM TPA dissolved in 100 mM pH 6.9 phosphate buffer solution, and then various voltages (E_{tot}) were applied across the channel. The one-electron oxidation of $Ru(bpy)_3^{2+}$ at the anode was designed to lead to emission of light via ECL, which provides a convenient probe of E_{crit}; that is, ECL will be observed when $\Delta E_{elec} > E_{crit}$.

Table 1

E_{tot} (V)	electric field (V/cm)	ΔE_{elec} (V) (500/450/400 μm)[a]	length of ECL illumination[b] (μm) (500/450/400 μm)[a]
55 (b)[c]	46	2.3/2.1/1.8	45/10/0
60 (c)	50	2.5/2.3/2.0	65/45/0
65 (d)	54	2.7/2.4/2.2	80/50/10
90 (e)	75	3.8/3.4/3.0	125/100/70
100 (f)	83	4.2/3.8/3.3	135/115/80

[a] These values refer to the lengths of the three intrachannel electrodes. [b] These values refer to the distance from the end of the anode toward the center of the conductor over which light is detected. [c] The letters refer to the panels in Figure 1 from which these data were derived.

Figure 1b shows the three-electrode array when $E_{tot} = 55$ V. ΔE_{elec} values of 1.8, 2.1, and 2.3 V were calculated for electrodes 400, 450, and 500 μm in length, respectively, using the expression $\Delta E_{elec} = dE/dx \times L_{elec}$. Under these conditions, the 500 μm microelectrode emits an easily detectable luminescent signal, light from the 450 μm electrode is barely detectable, and no light is present at the anode end of the 400 μm electrode. When E_{tot} is increased to 60 V, light emission is clearly observed at the 450 μm electrode (Figure 1c, $\Delta E_{elec} = 2.3$ V) but not at the 400 μm electrode ($\Delta E_{elec} = 2.0$ V). Note that light emission from the 500 μm electrode now extends further toward the center of the bipolar electrode than it did at $E_{tot} = 55$ V, indicating that a potential difference sufficient to drive the necessary faradaic processes extends further onto the electrode. Here, we begin to see one of the interesting aspects of this system: the illuminated length of the electrode is a function of both ΔE_{elec} and E_{crit} and thus represents a means for quantifying the reporter output. The 400 μm electrode remains dark under these conditions.

Further increases in ΔE_{elec} result in lengthening of the emission signatures on both the 500 and the 450 μm electrodes as ΔE_{elec} increases to 2.7 and 2.4 V, respectively, while luminescence from the shortest electrode ($\Delta E_{elec} = 2.2$ V) is weak but still detectable (Figure 1d). Results obtained for higher values of ΔE_{elec} confirm this general trend (Table 1, and Figure 1e and f). Importantly, as the potential increases, light emission expands along the long axis of the electrode, implying that for every position along the electrode, there is a different potential driving the ECL reaction.

In a second experiment, we recorded the entire ECL spectrum as a function of ΔE_{elec} for a single 500 μm bipolar electrode (Figure 2). The shape of these emission spectra is consistent with previous reports for this ECL system.[11] The trend toward higher emission intensity as a function of ΔE_{elec} (Figure 2b) corroborates the results shown in Figure 1: higher ΔE_{elec} leads to higher ECL intensities.

There are some important advantages of performing this sort of experiment using a two- or three-electrode configuration. To demonstrate this, we fabricated a two-electrode microfluidic device analogous to the just-described one-conductor system. It consists of a microfluidic device housing two 50-μm wide ITO electrodes oriented perpendicular to the channel and

(14) Duval, J.; Kleijn, J. M.; van Leeuwen, H. P. *J. Electroanal. Chem.* **2001**, *505*, 1−11.
(15) Fleischmann, M.; Ghoroghchian, J.; Rolison, D. R.; Pons, S. *J. Phys. Chem.* **1986**, *90*, 6392−6400.

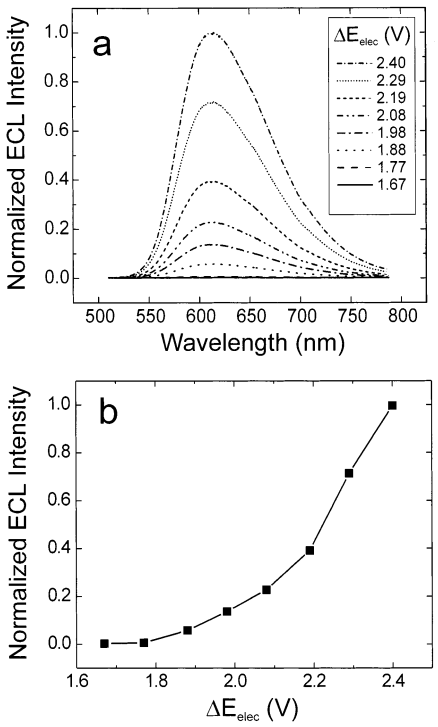

Figure 2. (a) Normalized ECL spectra, obtained using the wireless bipolar electrode configuration shown at the top of Scheme 1, as a function of the potential difference between the ends of the electrode (ΔE_{elec}). (b) Normalized ECL intensity at $\lambda_{max} = 610$ nm as a function of ΔE_{elec}. Data were obtained using a 500 μm-long ITO electrode. The 0.1 M phosphate buffer electrolyte solution (pH 6.9) contained 5 mM $Ru(bpy)_3^{2+}$ and 25 mM TPA.

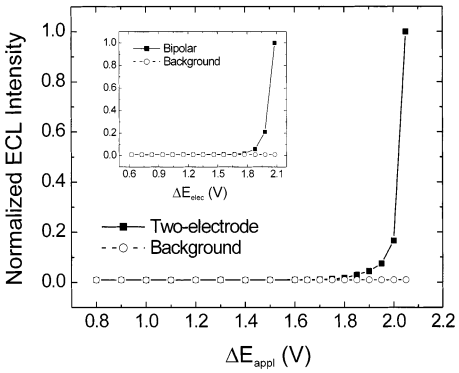

Figure 3. Normalized ECL intensities (at $\lambda_{max} = 610$ nm) as a function of ΔE_{appl} for the two-electrode configuration (bottom of Scheme 1). The inset shows analogous data for the single, bipolar electrode configuration. The 0.1 M phosphate buffer electrolyte solution (pH 6.9) contained 5 mM $Ru(bpy)_3^{2+}$ and 25 mM TPA. The background data were obtained in the absence of $Ru(bpy)_3^{2+}$ and TPA.

separated by a 400 μm gap. Scheme 1 compares this configuration to that of the bipolar electrode arrangement. Emission spectra obtained using the two-electrode cell were the same as those shown in Figure 2 when the potential applied between the two electrodes reached a value sufficient to drive the ECL reaction at the anode. Figure 3 compares the maximum ECL emission intensity for the bipolar and two-electrode configurations at $\lambda_{max} = 610$ nm as a function of ΔE_{appl} (the distance between the two electrodes was taken as that between the outer edges) and ΔE_{elec}, respectively. In both cases, ECL emission is first observed at ~1.8 V.[16] Background signals were obtained by collecting spectra under similar conditions, that is, at the same value of ΔE_{elec} or ΔE_{appl} and with the same data acquisition time, but in the absence of $Ru(bpy)_3^{2+}$ and TPA.

Scheme 3

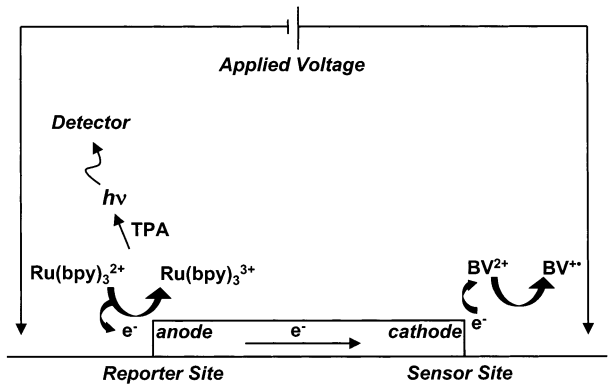

Electrochemical Sensing and Photonic Reporting from a Bipolar Electrode. As mentioned earlier, electrochemical processes occurring at the anode and cathode of either the bipolar or the two-electrode configuration (Scheme 1) are linked electrically but not chemically. That is, there is a one-to-one correspondence between the number of electrons consumed at the anode and the number provided at the cathode. In this section, we demonstrate that this observation provides a new way of thinking about electrochemical sensor design. Specifically, we show that electrochemical reactions occurring at the cathode of a one- or two-conductor cell can be followed by observing the ECL intensity at the anode. The principle of the single-electrode version of this system is illustrated in Scheme 3.

To demonstrate this dual sensing/reporting function, we compared the $Ru(bpy)_3^{2+}$ ECL intensity at the anode for the cathodic processes shown in eqs 1 and 2 (BV^{2+} is the benzyl viologen dication).

$$2H^+ + 2e = H_2 \qquad (E_1^{\circ\prime}) \tag{1}$$

$$BV^{2+} + e = BV^{+\cdot} \qquad (E_2^{\circ\prime}) \tag{2}$$

The formal potential for proton reduction ($E_1^{\circ\prime}$) occurs at a more negative potential than BV^{2+} reduction ($E_2^{\circ\prime}$) under the conditions used in these experiments (ITO working electrode, 5 mM $Ru(bpy)_3^{2+}$, 5 mM BV^{2+}, and 25 mM TPA in pH 6.9 aqueous 0.1 M phosphate buffer solution). This assertion is confirmed by the two voltammograms shown in Figure 4, which were obtained using a three-electrode cell having an ITO working electrode (area = 0.26 cm^2) and an Ag/AgCl (3 M NaCl) reference electrode. The shape of these voltammograms, especially the catalytic process occurring at positive potentials, is typical of the ECL reaction used in this study.[11] Reduction of BV^{2+} (voltammogram b) begins at about −0.52 V, while proton reduction is first observed at about −1.08 V (voltammogram a). The important point is that the potential window between the anodic process (ECL), which is the same for both voltammograms, and the corresponding cathodic reactions is different: in the presence of BV^{2+}, the voltage difference between

(16) The CCD-based photodetector used to obtain the luminescence data shown in Figures 2−7 was more sensitive than the camera (Nikon N2000) used to record the micrographs shown in Figure 1. Therefore, the minimum value of ΔE_{elec} necessary to detect luminescence is lower for the more sensitive detector.

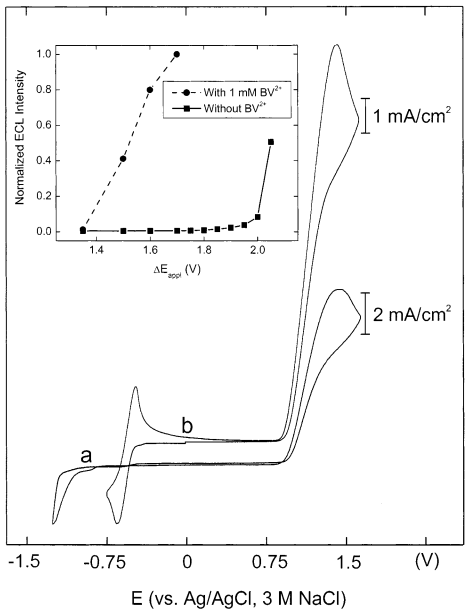

Figure 4. Cyclic voltammograms obtained using a conventional three-electrode cell. The 0.1 M phosphate buffer electrolyte solution (pH 6.9) contained 5 mM $Ru(bpy)_3^{2+}$ and 25 mM TPA. (a) In the absence of BV^{2+}. (b) In the presence of 1 mM BV^{2+}. The ITO working electrode had an area of 0.26 cm^2, and the scan rate was 100 mV/s. The inset shows the normalized ECL intensity at $\lambda_{max} = 610$ nm as a function of ΔE_{appl}. These data were collected using the two-electrode configuration shown at the bottom of Scheme 1 and the same electrolyte solution used to obtain the voltammograms.

the onset of the cathodic and anodic processes narrows from 1.80 to about 1.38 V.

The inset of Figure 4 compares the voltammetry to the ECL intensities observed for the two-electrode configuration. When BV^{2+} is introduced into the microfluidic channel, ECL is readily observed at $\Delta E_{appl} = 1.4$ V, which correlates well to the 1.38 V window between the anodic and cathodic processes for voltammogram b. At 1.8 V, the potential at which ECL is just starting to turn on for the cathode reaction corresponding to eq 1, a very large luminescent intensity is observed for the BV^{2+}-containing solution. Specifically, when 100 μM BV^{2+} was added to a solution containing 5 mM $Ru(bpy)_3^{2+}$ and 25 mM TPA, a 40-fold enhancement in the ECL intensity was observed at $\lambda_{max} = 610$ nm for $\Delta E_{elec} = 1.7$ V. Although detecting BV^{2+} is not a technically demanding task, this example conclusively demonstrates the relationship between the sensing and reporting functions of this sensor, and that it can distinguish between two different targets on the basis of their redox potentials.

Next, we explored how ECL intensity varies as a function of the concentration of BV^{2+} present in the microfluidic channel and as a function of the bias voltage applied between the two electrodes. Independent of potential, the maximum luminescence signal was observed at a BV^{2+} concentration of 100 μM (Figure 5). The increase leading up to this point is easy to understand: a higher concentration of BV^{2+} leads to a larger cathodic current and, because of charge balance, a correspondingly high anodic current, which in turn drives the ECL reaction faster. A concentration of BV^{2+} of 100 nM was easily detected, and by using a more sensitive photodetector, it should be possible to reduce this value significantly.

The decrease in emission intensity observed at concentrations higher than 100 μM is due to either the cross-reaction between

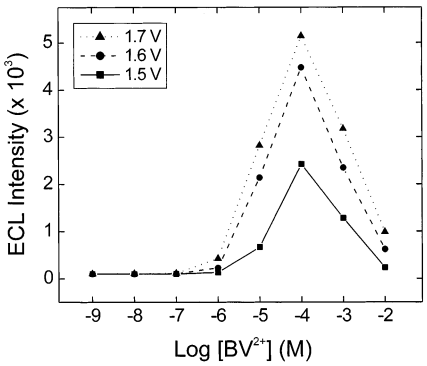

Figure 5. ECL intensity at $\lambda_{max} = 610$ nm as a function of BV^{2+} concentration. Data were collected using the two-electrode configuration shown at the bottom of Scheme 1. The 0.1 M phosphate buffer electrolyte solution (pH 6.9) contained 5 mM $Ru(bpy)_3^{2+}$ and 25 mM TPA.

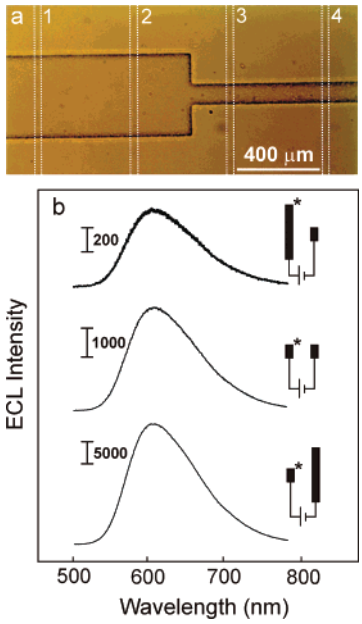

Figure 6. Effect of electrode area on ECL intensity for the two-electrode configuration shown at the bottom of Scheme 1. (a) Optical micrograph of the microfluidic device used to obtain the data. The numbered electrodes are highlighted with dashed white lines because of poor optical contrast between ITO electrodes and the glass substrate. The available area for the electrochemical reaction is defined by the width of the ITO electrodes (50 μm) and the width of the channel (for electrodes 1 and 2, 400 μm; for electrodes 3 and 4, 100 μm). (b) ECL spectra obtained as a function of the relative area of the anode and cathode. The three configurations studied are illustrated to the right of the spectra. For the upper and lower spectra, electrodes 2 and 3 were used, and for the middle spectrum, electrodes 1 and 2 were connected. Light was collected from the anode, which is indicated by an asterisk. In each case, $\Delta E_{appl} = 1.95$ V. The 0.1 M phosphate buffer electrolyte solution (pH 6.9) contained 5 mM $Ru(bpy)_3^{2+}$ and 25 mM TPA (but not BV^{2+}).

$BV^{+\cdot}$ and $Ru(bpy)_3^{3+}$ or quenching of the excited state of $Ru(bpy)_3^{2+}$ by $BV^{+\cdot}$. Both of these processes are a consequence of the close proximity of the anode and cathode (less than 500 μm, Scheme 1). We have demonstrated this to be the case by separating the anode and cathode reactions into different microfluidic channels; these results will be reported elsewhere.[2]

ECL Intensity as a Function of the Relative Areas of the Anode and Cathode of the Bipolar Electrode. Thus far, we have demonstrated that ECL intensity increases as a function of increasing potential difference between the anode and cathode and as a function of the concentration of the electrochemical

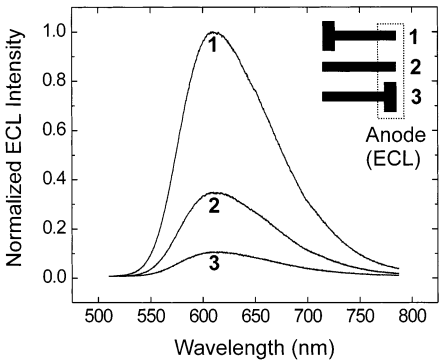

Figure 7. ECL spectra obtained as a function of the relative area of the anode and cathode for the bipolar (one-electrode) configuration shown at the top of Scheme 1. The three configurations studied are illustrated to the right of the spectra. The length of each electrode was 500 μm. The wide ends of electrodes 1 and 3 were 200 μm $\times$ 100 μm. The thin ends of the electrodes were 50 μm in width. In each case, $\Delta E_{elec} = 1.88$ V. The 0.1 M phosphate buffer electrolyte solution (pH 6.9) contained 5 mM $Ru(bpy)_3^{2+}$ and 25 mM TPA (but not BV^{2+}).

target reduced at the cathode. Indeed, it is obvious that any experimental condition that produces more current at the cathode will enhance the ECL intensity at the anode. Accordingly, we anticipated that under otherwise identical conditions, increasing the area of the cathode relative to the anode would result in more intense ECL. To test this hypothesis, we measured ECL intensity as a function of the relative areas of the cathode and anode using the two-electrode configuration.

Figure 6a is an optical micrograph of a microfluidic channel incorporating four ITO band electrodes configured perpendicular to the channel. The electrodes, numbered 1−4, are outlined with dashed white lines because of poor optical contrast between the glass substrate and the ITO. Because the fluidic channel is designed to be narrower on the right side than on the left, the areas of electrodes 1 and 2 are 4 times larger than the areas of electrodes 3 and 4. When a 1.95 V bias is applied between electrodes having the same area (either electrodes 1 and 2 or electrodes 3 and 4), ECL spectra exhibiting the same maximum intensity are observed (one such spectrum is shown in the middle of Figure 6b). However, when electrode 2 was connected as the anode and electrode 3 as the cathode, a decrease in the ECL intensity was observed at electrode 2 (top of Figure 6b). This occurs because the absolute number of electrons moving out of the cathode (and thus into the anode) is proportional to the cathode area. Similarly, when the same two electrodes were connected, but the anode and cathode reversed (bottom of Figure 6b), the ECL intensity at the maximum emission wavelength (610 nm) was enhanced by more than a factor of 6 as compared to the case when both electrodes have the same area.

This same area-dependent effect is observed for the bipolar electrode configuration (Figure 7). Here, ECL spectra from two T-shaped electrodes are compared to a band electrode having equal areas at the two ends. The highest ECL intensity is observed when the area of the cathode is large relative to the anode.

Summary and Conclusions

The results reported here provide a means to detect electrochemical events and report them photonically regardless of whether the electroactive analyte participates in the ECL reaction sequence. This greatly increases the number of analytes that can be detected using the highly sensitive ECL process. Importantly, the anode and cathode reactions are coupled electrically, and therefore it is possible to correlate ECL intensity to the concentration of the reduced analyte, thereby quantifying it. We also showed that by changing the shape of the anode and cathode relative to one another, it is possible to enhance the sensitivity of the method.

In addition to decoupling the chemistry of the sensing and reporting functions of this sensor, the ability of the system to operate with a single bipolar electrode having no external electrical contacts is important.[4] For example, by using bipolar electrodes of differing lengths, it is possible to create electrode arrays that are sensitive to targets whose half reactions have different formal potentials. We showed that such a device could be read out by measuring either the intensity of the ECL or the length of the electrode that is illuminated. In the two-electrode configuration, such a device could easily be miniaturized with a small battery providing the necessary power and a photodiode collecting the light emission. We envision that this same approach will be used to build more sophisticated sensors. One approach might involve immobilization of selective receptors, already devised for other electrochemical sensor applications, on the cathode. It is also easy to imagine constructing more versatile devices containing many channels, each of which contains many electrodes that can detect different analytes.

Acknowledgment. We gratefully acknowledge financial support from the Office of Naval Research, the U.S. Army Medical Research and Material Command, and the Texas Higher Education Coordinating Board through the Advanced Technology Program (0082-1999). We also thank the following individuals who helped us to conceive of this work and interpret the results: Professor Allen J. Bard (University of Texas), Dr. Antonio J. Ricco and Dr. Minq-qi Zhao (ACLARA BioSciences, Mountain View, CA), Dr. Li Sun (Texas A&M University), and Professor Henry S. White (University of Utah). Some of the instrumentation used to carry out this work was provided by the Center for Integrated Microchemical Systems at Texas A&M University.

JA020907S